The EMBO Journal (2013) 32, 3096–3105
www.embojournal.org

TRANSPARENT PROCESS

THE EMBO JOURNAL

Structural evidence for functional lipid interactions in the betaine transporter BetP

Caroline Koshy[1], Eva S Schweikhard[1], Rebecca M Gärtner[1], Camilo Perez[1], Özkan Yildiz[1] and Christine Ziegler[1,2,*]

[1]Department of Structural Biology, Max-Planck Institute of Biophysics, Frankfurt am Main, Germany and [2]Department of Protein Crystallography, Institute of Biophysics and Biophysical Chemistry, University of Regensburg, Regensburg, Germany

Bilayer lipids contribute to the stability of membrane transporters and are crucially involved in their proper functioning. However, the molecular knowledge of how surrounding lipids affect membrane transport is surprisingly limited and despite its general importance is rarely considered in the molecular description of a transport mechanism. One reason is that only few atomic resolution structures of channels or transporters reveal a functional interaction with lipids, which are difficult to detect in X-ray structures *per se*. Overcoming these difficulties, we report here on a new structure of the osmotic stress-regulated betaine transporter BetP in complex with anionic lipids. This lipid-associated BetP structure is important in the molecular understanding of osmoregulation due to the strong dependence of activity regulation in BetP on the presence of negatively charged lipids. We detected eight resolved palmitoyl-oleoyl phosphatidyl glycerol (PG) lipids mimicking parts of the membrane leaflets and interacting with key residues in transport and regulation. The lipid–protein interactions observed here in structural detail in BetP provide molecular insights into the role of lipids in osmoregulated secondary transport.

The EMBO Journal (2013) **32,** 3096–3105. doi:10.1038/emboj.2013.226; Published online 18 October 2013
Subject Categories: membranes & transport; structural biology
Keywords: atomic structure; lipid–protein interaction; osmotic stress; secondary transport; transport regulation

Introduction

Transmembrane proteins need to function in a fluid lipid bilayer environment. Over the years, many observations have indicated that the bilayer often plays an essential part in the organization and function of membrane proteins (Lee, 2004; Phillips *et al*, 2009). Specific bilayer lipids can be essential cofactors for proteins in folding and function, as seen in the crystal structure of the potassium channel KcsA (Zhou *et al*, 2001; Valiyaveetil *et al*, 2002). Membrane lipids can control function by deforming locally to compensate for the hydrophobic mismatch between protein and bilayer thickness, as in the gating of bacterial mechanosensitive channels, which respond to membrane mechanical stress (Perozo *et al*, 2002; Phillips *et al*, 2009). Lipid head-group compositions have also been shown to influence the activity of proteins like the diacylglycerol kinases and cation-pumping ATPases (Lee, 1998, 2004; Quick *et al*, 2012). Recently, experimental and computational studies on the secondary transporter LeuT indicated that the surrounding environment (detergent micelle or lipid bicelle) could play an important role in its function (Zhao *et al*, 2011; Quick *et al*, 2012; Wang *et al*, 2012). The membrane environment of LeuT was further shown to respond dynamically to the structural features of conformational changes in this transporter, by computational studies (Mondal *et al*, 2013). LeuT is an important prototype for secondary transport in that many functionally unrelated transporters share its fold (Forrest *et al*, 2011).

The betaine symporter BetP is one such secondary transporter, which shares the conserved LeuT-like fold of two structurally related, topologically inverted domains (Supplementary Figure S1a and b). It is a key player in the hyperosmotic stress response of *Corynebacterium glutamicum* (Peter *et al*, 1996; Morbach and Krämer, 2003; Krämer and Morbach, 2004). This soil bacterium exhibits a very uncommon plasma membrane composition comprising lipids with only negatively charged head groups namely phosphotidyl glycerol (PG), phosphotidyl inositol (PI) and cardiolipin (CL), with exclusively 16:0/18:1 fatty acyl chains (Hoischen and Krämer, 1990; Schiller *et al*, 2006; Özcan *et al*, 2007). Regulation of transport activity in BetP is triggered by an increase in the internal concentrations of K^+ in hyperosmotic stress situations (Rübenhagen *et al*, 2001). The response of betaine uptake rate to increasing external osmolality is severely compromised in membranes lacking negatively charged lipids (Rübenhagen *et al*, 2000; Schiller *et al*, 2006). Its activation optimum also crucially depends on the fraction of 16:0/18:1 fatty acyl chains (Özcan *et al*, 2007). It has been suggested that BetP is able to sense stress and achieve full activity at low temperatures *via* a signal that stems directly from the membrane (Özcan *et al*, 2005). Structural data obtained from BetP reconstituted in 2D crystals implied that these might include changes in membrane curvature or thickness (Tsai *et al*, 2011). This as yet undefined lipid–protein interaction is an intriguing proposition because other osmotic stress-regulated transporters (van der Heide *et al*, 2001; Poolman *et al*, 2004) also depend on the presence of specific lipids for their optimal activation. In fact, lipid–protein interactions are often found in stress-triggered activation, for example, during salt stress to affect water transport via aquaporins (Walz *et al*, 1997) or during hypotonic stress to activate mechanosensitive channels (Yoshimura and Sokabe, 2010). The stringent causality between transport regulation of BetP and the unique

*Corresponding author. Department of Structural Biology, Max-Planck Institute of Biophysics, Max-von-Laue Strasse 3, 60438 Frankfurt, Germany. Tel.: +49 69 6303 3054; Fax: +49 69 6303 2209; E-mail: christine.ziegler@biophys.mpg.de

Received: 6 May 2013; accepted: 11 September 2013; published online: 18 October 2013

composition of the *C. glutamicum* membrane (Özcan *et al*, 2007) coupled with the wealth of structural data makes BetP a prime example to structurally investigate regulatory lipid–protein interactions. Atomic structures of BetP in different conformational states allowed recently for the molecular description of the alternating access cycle of BetP that involves a hinge-like gating movement along the midsection of mainly two transmembrane helices from each inverted repeat, TM1′ (The numbering of the BetP TM helices was adapted to the LeuT numbering for better comparison. Therefore, TM1′–TM10′ correspond to TM3–TM12, while TM1 and TM2 are now assigned as TM(−2) and TM(−1), respectively; Supplementary Figure S1c.) and TM5′ to open the cytoplasmic pathway and TM6′ and TM10′ to open the periplasmic pathway (Perez *et al*, 2012; Figure 1B). These structures unambiguously identified key players in the co-transport of sodium and betaine.

Here, we describe a new X-ray structure of a BetP trimer, in which all three protomers adopt a similar inward-facing state resolved to 2.7 Å with specifically bound PG lipids. The structure reveals in atomic detail how the gating helix TM1′ (Forrest *et al*, 2011), which also plays an important role in conformational changes in LeuT-like fold transporters, interacts with lipids. The observed lipid–protein interaction sites involving residues important in both transport and regulation of BetP highlight the functional impact of lipids in the structure-based transport mechanism of a LeuT-like fold transporter.

Results

Structure of BetP trimer with all three protomers in inward-facing state

We determined the crystal structure of a BetP trimer with each chain adopting an inward-open state (C_i) at a resolution of 2.7 Å (Figure 1A). This structure was obtained after removing unspecifically bound lipids by thorough washing steps during detergent exchange on the affinity column (Supplementary methods). Washing would also remove any endogeneous betaine that could bind in the structure and no external betaine was added during purification and crystallization. The main-chain conformations of the C_i state at 2.7 Å are identical to previously reported inward-facing substrate bound (C_iS) structures at lower resolution (Ressl *et al*, 2009; Perez *et al*, 2011b, 2012), which crystallized as asymmetric trimers with respect to their conformational state.

A citrate buffer molecule is wedged into the cytoplasmic funnel in all three chains, and is located below the central S1

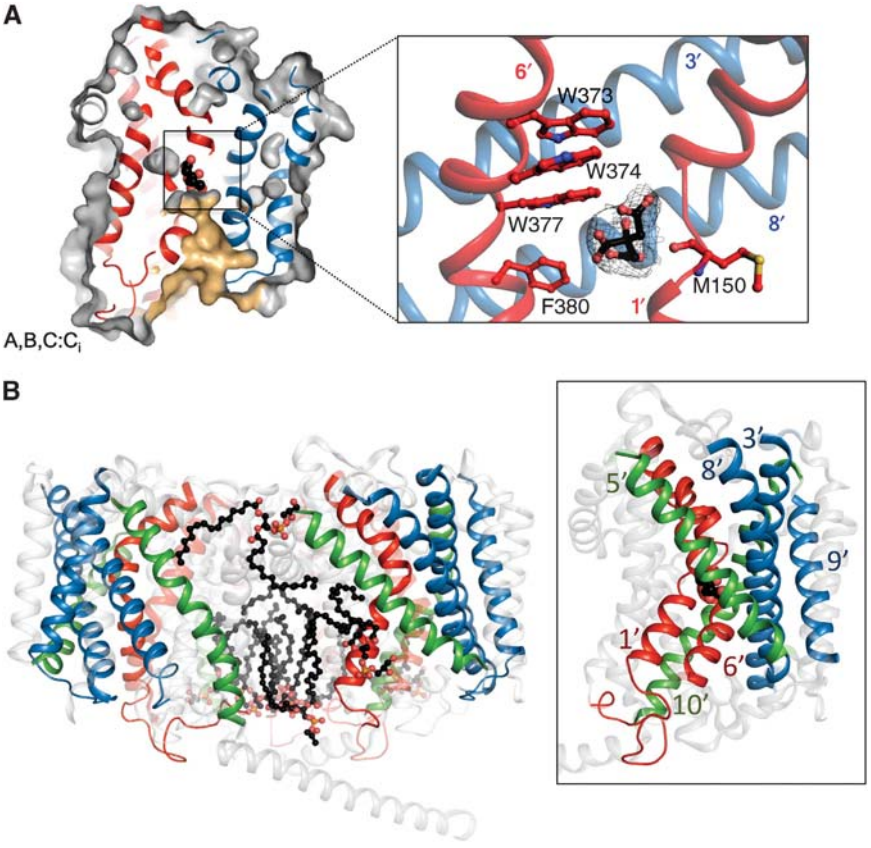

Figure 1 (**A**) Inward-open state of BetP at 2.7 Å: surface cut of the inward-open state (C_i) with citrate bound in the pathway, adopted by all three chains (A–C). The inset panel shows the functionally important and evolutionarily conserved tryptophans in TM6′—Trp373, Trp374 and Trp377, stacked like the rungs of a ladder in this conformation. The citrate buffer molecule is shown in black stick representation with the 2Fo-Fc map for citrate contoured at 1σ. This site is occupied by choline and betaine in previously reported structures PDB: 3P03 at 3.3 Å and PDB: 4AIN at 3.1 Å resolution, respectively. (**B**) Resolved lipids are shown in trimeric context with helices of each chain involved in conformational changes highlighted. Lipids are closely associated with loops connecting helices involved in functional movement. Inset shows distinct elements in the conformational changes in BetP during the alternating access mechanism for substrate translocation. Bundle helices are in red, scaffold helices in blue and arm helices in green. The cytoplasmic halves of TM1′ and 5′ are the gating elements for the inward opening of the transporter while their symmetry equivalents TM6′ and TM10′ gate the periplasmic opening.

substrate-binding site that was described previously in betaine-bound closed-state structures (Perez *et al*, 2012). It is coordinated at a similar site between TM1′ and TM6′ as betaine (Perez *et al*, 2012) or choline (Perez *et al*, 2011b, 2012) in previously reported structures of inward-open substrate bound conformations, although it has no functional impact on BetP, that is, as an inhibitor or a competitor for betaine (data not shown). Although the transporter state is identical in all there protomers, each chain differs in the folding and orientation of its C-terminal domain that forms an α-helix in chains A and C (Supplementary Figure S3). The C-terminal helix contains a zipper-like arrangement of several arginines that are crucial in stress sensing and regulation (Ott *et al*, 2008). In chain B only a few residues are resolved, reflecting its flexibility. In its helical arrangement, the C-terminal domain interacts with loop 2 of the adjacent chain establishing the cytoplasmic network (Ressl *et al*, 2009) for which the C-terminal domain of chain A interacts with loop 2 of chain C, while the C-terminal domain of chain C interacts with loop 2 in chain B (Supplementary Figure S3b and c). The structurally observed interaction sites are in good agreement with mutagenesis studies (Ott *et al*, 2008) and especially restrict the gating helices TM1′ and TM6′ on the cytoplasmic side of chains B and C.

Lipid densities resolved in the BetP trimer

The improved resolution crystals of BetP revealed strong elongated densities in the Fo-Fc map, which could be assigned to lipid moieties (Supplementary Figure S4). From the observed densities, the most easily identified were used to build lipid chains into the model during refinement, after having systematically excluded other possibilities like detergents from the crystallization conditions. Specifically, they correspond to eight ordered lipids bound to the BetP trimer. The head groups of the lipids could be identified and the acyl chains are resolved almost completely along their entire length, even at a modest resolution of 2.7 Å, albeit with different levels of flexibility, suggesting that these lipids are reasonably well ordered. Head groups were assigned to negatively charged phosphatidyl glycerol (PG) based on the 2Fo-Fc and Fo-Fc difference maps as well as the mainly positively charged residues coordinating them (Figures 2–4; Supplementary Figure S4). The extent of the densities in the 2Fo-Fc maps additionally argued for the placement of the longer PG heads as opposed to the shorter phosphatidyl ethanolamine (PE) head group and model building with the latter led to unsatisfied head-group electron densities. Cardiolipin, which is the other predominant negatively charged lipid in the *C. glutamicum* lipidome and also a component in the *E. coli* membrane, was also tested. However, model building with cardiolipin resulted in unconvincing fitting of densities at head-group position and was subsequently excluded. Although given the resolution there is ambiguity in assigning the correct acyl chains, the extended densities in the structure best fitted a 16/18 acyl chain length during refinement. The major 16/18 acyl chain composition of PG lipids in the phospholipidome of the heterologous expression system *E. coli* has been identified by mass spectrometric analysis as 16:0/18:1 (Oursel *et al*, 2007; Matyash *et al*, 2008). Consequently, we assigned the acyl chains of the identified lipids to 16:0 palmitoleyl–18:1 oleoyl.

Lipid analysis of purified BetP by thin layer chromatography identifies PG

In order to resolve any ambiguity in lipid assignment in the structure given the modest resolution, we performed TLC on BetP protein prepared for crystallization. Chromatography using different solvent systems enabled the detection of phospholipids in BetP. An initial one-dimensional separation clearly excluded the presence of positively charged PE from the protein sample (Supplementary Figure S5a) and showed the presence of negatively charged CL/PG species. However, interpretation was confounded since Cymal-5, the detergent in BetP, also runs at the same height (Supplementary Figure S5a and b). The negatively charged species was further separated using an acetone:acetic acid:water:methanol system (Supplementary methods). In this 1D separation run, a phospholipid spot in BetP co-migrating with the PG standard was observed (Supplementary Figure S5b), indicating the presence of anionic PG lipids in purified BetP. No distinct CL species could be identified, but the possibility of some amounts of the cardiolipin being present and migrating at the same height as the Cymal-5 spot could not be eliminated. Although cardiolipin could not be identified from the better-resolved lipid densities within the structure, it may well be a component of the annular lipids present along the periphery of the trimer.

Eight POPG binding sites within trimeric BetP

The lipids are resolved along the membrane limits (Supplementary Figure S6) with seven lipids aligned with the lower (L1–7) cytoplasmic leaflet and one lipid resolved from the upper (U1) periplasmic membrane leaflet. Five of these lipids are non-annular and appear to mediate intra-trimeric contacts in the BetP core (Figure 2A and B). Three other lipids are annular, present on the outer surface of the protein (Figures 3, 4A and B). These lipids are less well ordered reflecting the faster exchange of lipids on the surface with those in the membrane bulk (Lee, 2011) while electron densities for the non-annular lipids are better resolved, presumably due to their restriction within the trimer. Consequently, the assignment of annular lipids to PG was based mainly on the extent of densities for the head groups.

Three completely resolved lipid molecules (L1–3) are present in the trimer centre, each coordinated by residues from adjacent chains (Figure 2A). Positively charged residues from loop 2 (Lys121) and internal loop IL3 (Arg395) from adjacent chains coordinate these lipid moieties, which are resolved at symmetric sites within the trimer (Figure 5A). L1 extends between chains A and B, whereas L2 and L3 are coordinated by chains B-C and A-C, respectively (Figure 2B).

Lipid molecule L4 mediates a cytoplasmic interaction network, involving the longest resolved C-terminal helix of chain A and loops from adjacent chains. Positively charged residues from loops 2 (Arg126) and IL3 (Arg395) in chain C and the C-terminal domain of chain A (Arg554, Arg558 and side chain -NH of Gln557) coordinate the negatively charged head group of L4 (Figure 2B). The corresponding lipid position between loops 2 and IL3 is not occupied between chains A and B, since the C-terminal domain of chain B is flexible and not resolved in the structure. Some density consistent with a lipid head group is present between chains B and C at this position, but was not modelled in the structure due to its limited resolution.

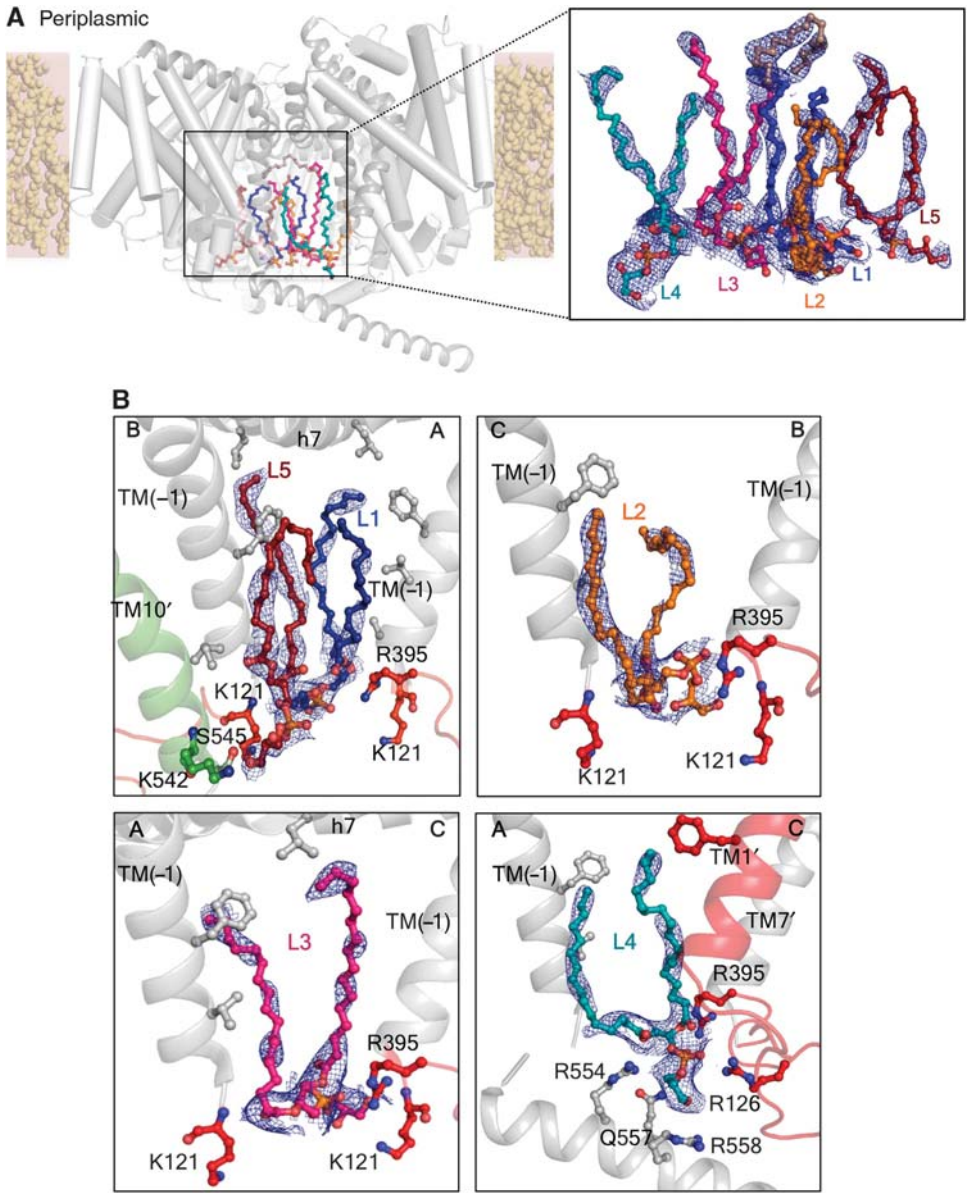

Figure 2 Non-annular lipids: (**A**) Membrane view of lipids bound in the centre of the trimer with helices providing co-ordination residues shown as grey oval helices, while the rest of the trimer is shown as cylindrical helices. The inset figure shows five completely resolved POPG lipids L1–L5 in stick representations. An acyl chain for which no head-group density was resolved is shown in dark salmon. The final 2Fo-Fc maps for the lipids (which were modelled after multiple iterative rounds of refinement prior to placement indicated their positions) are contoured at 0.8σ. (**B**) Detailed residue coordination for each non-annular lipid: coordinating helices that are also involved in conformational changes are coloured according to Figure 1B, in order to recognize regions that are both membrane associated and part of the dynamics of the transport cycle. The head group of lipid L1 is coordinated by K121 (loop 2) and R395 (IL3) from chain A and main chain carbonyl of K121 from chain B. Head group of L5 is coordinated by K542 and S545 of chain B. Coordination for the head group of L2 is via K121 (loop 2-chain C), K121 (loop 2-chain B) and R395 (IL3-chain B). L3 is similarly coordinated by K121 (loop 2-chain A), K121 (loop 2-chain C) and R395 (IL3-chain C). POPG head group for L4 is coordinated between R554, R558, Q557 (C-terminal helix-chain A), R126 (loop 2-chain C) and R395 (IL3-chain C). The acyl chains of these lipids are coordinated by hydrophobic residues from helices lining the trimer core and are shown in stick representations.

The acyl chains of L1, L2, L3 and L4 (Figure 2A and B) extend into the central core of the trimer and are coordinated by hydrophobic side chains from TM(−1), TM10′, TM7′, TM1′ and h7 the amphipathic helix unique to the Betaine-Choline-Carnitine Transporter (BCCT) family (Ziegler *et al*, 2010), lying parallel to the membrane (Figure 2B; Supplementary Figures S2 and S9). A single acyl chain for which head group is not resolved is also observed in the centre of the trimer coordinated by h7, forming a lipid plug between the chains (Figure 2A and inset).

Lipid L5 is resolved close to the trimer core between chains A and B and is coordinated by residues in the loop preceding the C-terminal domain of chain B, namely Lys542 and Ser545. Some density is observed at the same site between chains A and C, which might correspond to a lipid head group, but was not modelled in due to the ambiguity. Peripheral lipid molecule L6 is resolved close to this site between chains C and B, coordinated by residues from chain C's TM(−1) and TM10′—a key element in the conformational changes during transport (Perez *et al*, 2012) (Figure 3).

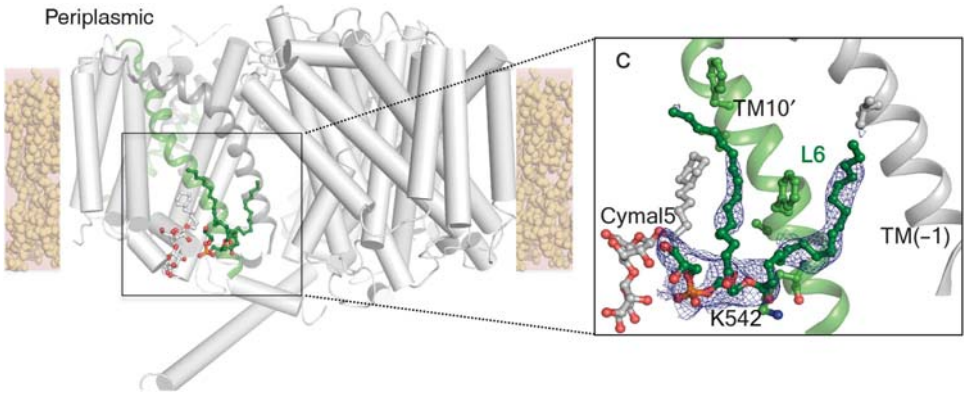

Figure 3 Annular lipids: Membrane view of lipid L6 resolved at the trimer periphery. The final 2Fo-Fc map density is contoured at 0.8σ. A Cymal5 molecule shown in grey provides additional head-group coordination for lipid L6 (inset).

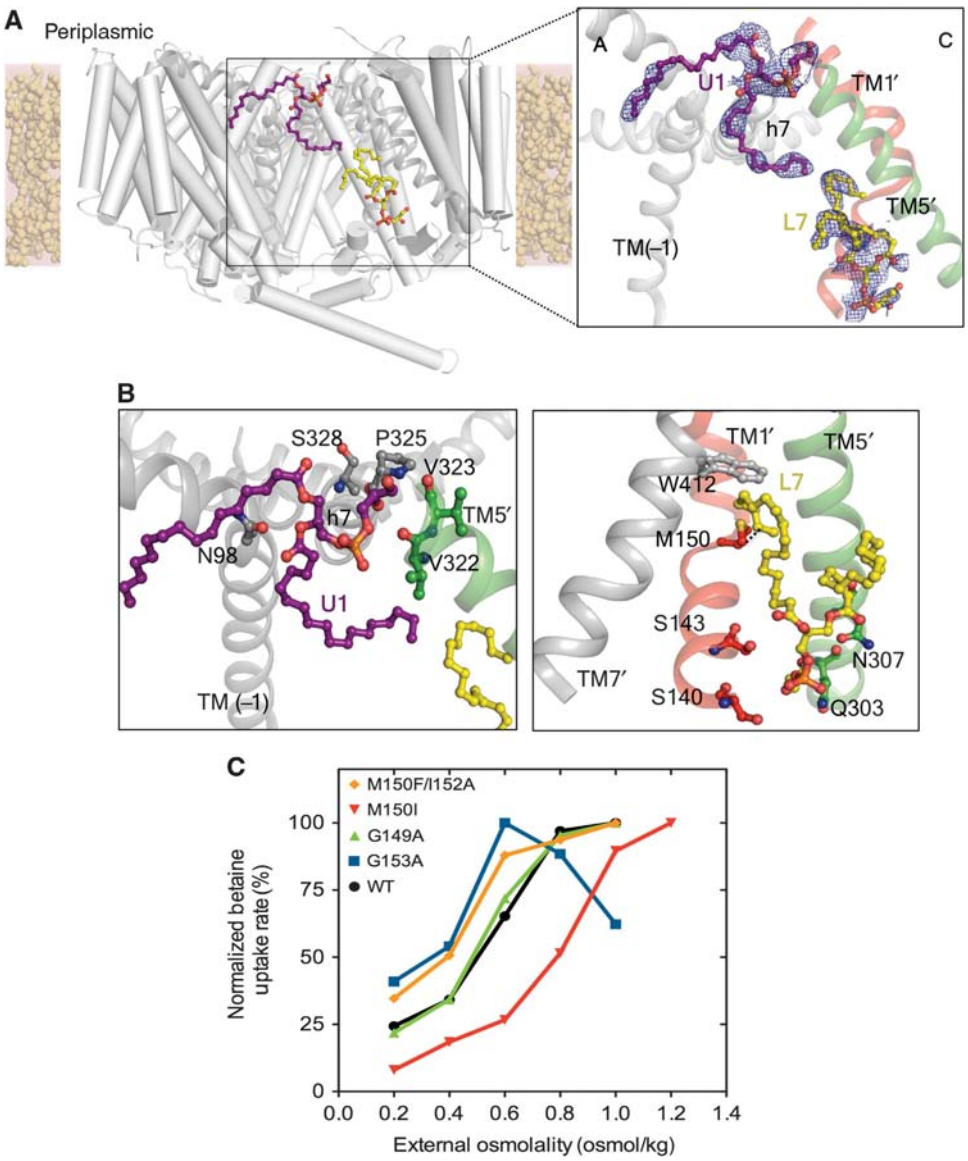

Figure 4 Annular lipids: (**A**) Membrane view of lipids U1and L7 resolved at the trimer periphery. Final 2Fo-Fc map densities are contoured at 0.8σ. (**B**) Detailed residue coordination for upper leaflet lipid U1 and lower leaflet lipid L7 is shown. Helices and residues involved in lipid coordination are highlighted and coloured according to Figure 1B if also involved in conformational changes. (**C**) Normalized activity regulation in BetP TM1′ unwound helix mutants in *E. coli* MKH13 cells: regulation of betaine uptake is shown for BetP WT (black circle/116.5 nmol/min × mg dw), BetP M150I (red triangles/75.6 nom/min × mg dw), BetP M150F/I152A (orange diamonds/146.9 nmol × mg dw) and stretch mutants BetP G149A (green triangles/38.1 nmol/min × mg dw) and BetP G153A (blue squares/45.2 nmol/min × mg dw). Normalization was carried out for each mutant related to its highest activity, indicated in parenthesis.

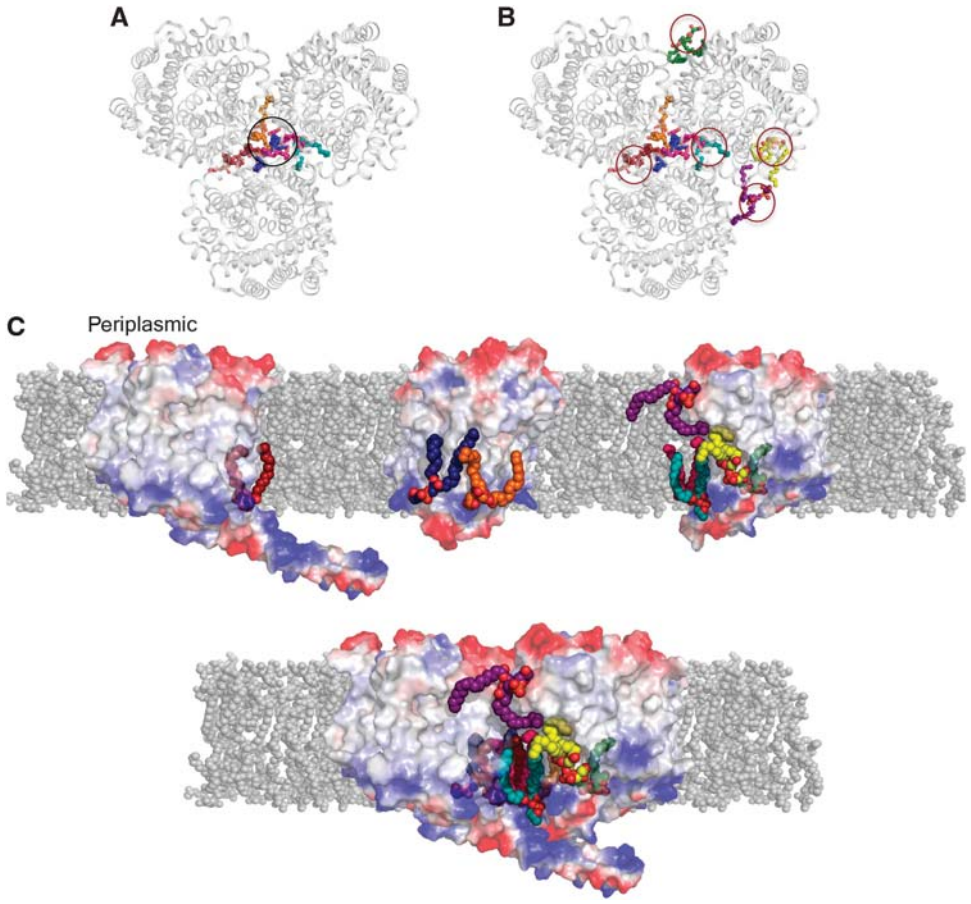

Figure 5 (**A**) L1, L2 and L3 marked in a black circle are resolved at symmetrical sites in the central hydrophobic cavity formed by the three chains. (**B**) L4, L5, L6, L7 and U1 (red circles) on the other hand do not have equivalently resolved lipid molecules in the trimer. (**C**) Asymmetrically occupied lipid-binding sites: membrane view of each monomer from the crystallized trimer showing lipids individually associated with it in spheres. The lipids are coloured according to Figures 2 and 3. Bulk lipids are shown in grey. In general, monomers in the membrane may have different lipid sites occupied. These bound lipids can serve as cofactors providing additional electrostatically favourable interaction sites for trimeric assembly (lower panel).

Another annular lipid L7 is resolved on the trimer periphery associated with residues on the cytoplasmic half of TM1′, which navigates the maximum movement in the inward opening of BetP (Perez *et al*, 2012) (Figure 4A and B). Some density which best fitted a lipid head group was resolved between residues from the periplasmic end of TM(−1) in chain A and amphipathic h7 from chain C (Figure 4A). The head group and acyl chains of this lipid (U1) from the upper membrane leaflet are also coordinated by residues from TM5′ of chain C. Density for acyl chains in this lipid is visible but flexible reflecting the lack of a distinct coordination. Both annular lipids, U1 and L7, are resolved close to symmetry molecules in the structure, which could influence their packing though they are not directly coordinated by crystal contacts (Supplementary Figure S10). Consequently, these lipid sites are asymmetrical and no corresponding lipid moieties are distinctly identifiable in other chains (Figure 5B).

One of the acyl chains of the annular lipid L7 accesses a hydrophobic cleft halfway through chain C lined by residues Val408 and Trp412 from TM7′ and Ala313, Ala314, Ala317 and Ile318 from TM5′ (Supplementary Figure S7). The tip of this acyl chain is involved in direct van der Waal's interactions with Met150 in the glycine-rich unwound region of TM1′ (Figure 4B). This stretch makes a 6-Å movement during conformational changes from outward to inward via the closed state (Supplementary Figure S11). Being an annular lipid, this moiety was recognized by patches of head-group density and acyl chain density close to the interaction site with the transporter.

Discussion

Structure of state-symmetric trimer reveals specific lipid binding

Compared to other LeuT-like fold transporters the cytoplasmic funnel in the inward-facing state of BetP is narrower (Perez *et al*, 2012). The C_i state was only observed in chain C in previously reported structures (Ressl *et al*, 2009; Perez *et al*, 2011b, 2012). This chain exhibits the closest contact with a C-terminal domain within the trimer, also the major crystal contact, and we could not exclude a restrictive effect on the cytoplasmic opening of BetP (Perez *et al*, 2012). Here, we observe a structurally identical inward-facing state also in chains B and A, the latter being free from any C-terminal interactions or crystal contacts, and thus demonstrate that the functional substrate-free open inward-facing (C_i) state of BetP is in fact narrower than in other LeuT-like fold transporters.

Therefore, with respect to the transporter states this new structure is the most symmetric of all BetP structures obtained thus far. It is also the one with the best resolution so far, which allowed us to identify eight PG lipid-binding sites within the trimer. Strikingly, negatively charged PG lipids constitute only 15% of the membrane fraction in the *E. coli* expression system whose major membrane component is PE (Rübenhagen *et al*, 2000), whereas PG is the major membrane component in *C. glutamicum* (Özcan *et al*, 2007). This implies that native lipids are selected for and retained during the heterologous expression, purification and crystallization of BetP emphasizing their structural necessity. The assignments to PG lipids are in perfect agreement with multiple biochemical and functional studies (Schiller *et al*, 2006; Özcan *et al*, 2007), all of which show that this lipid species is crucially involved in transport regulation in BetP.

Lipids associate with helices involved in conformational changes

Some of the resolved lipids are coordinated by residues from helices or loops involved in conformational changes. The head groups of all three of the lipids resolved at symmetric sites in the trimer centre L1–L3 (Figure 5A) are coordinated by residues from loops 2 and IL3. Both these loops link together functionally important helices. Loop 2 connects peripheral helix TM(−1) to TM1′, which is one of the gating elements opening the cytoplasmic half of BetP during transport (Perez *et al*, 2012). IL3 connects TM6′ and TM7′, which like TM1′, are also part of the 4TM bundle domain, containing within them the substrate translocation pathway (Perez *et al*, 2012). Previously, we showed that disruption of a cation-π interaction between residues from loops 2 and IL3 led to a dramatic decrease in activity and upregulation by osmotic stress was no longer possible (Gärtner *et al*, 2011). Therefore, between them, these two loops form an important lipid head-group coordination site. Lipid L4 in addition to being coordinated by loops 2 and IL3 also involves the C-terminal helix of chain A (Figure 2B). The negatively charged lipid molecule here provides an interaction site to effectively restrain the positively charged stretch in the C-terminal helix and consequently restrict movement of the loops connecting the bundle helices in a regulatory manner (Gärtner *et al*, 2011). To date, it is not known whether this regulatory restriction from the membrane results in upregulation or downregulation of the transport activity, which is attributed to the fact that mutations in the ionic network of loop 2 are not tolerated. However, having key components in the functional conformational changes directly accessible by the membrane may prove to be beneficial to communicate changes in the state of the membrane due to osmotic stress, an important factor in osmoregulation (Wood, 1999), through the core of the protein.

Structural interaction of annular lipid with the catalytic core

Lipid L7 is nested between TM5′ and TM1′, with one of its acyl chains interacting with the functionally important glycine-rich unwound stretch in TM1′ (Figure 4A and B). Along with being crucial in conformational changes, mutation of a glycine in this unfolded region to an aspartate was sufficient to alter substrate specificity in BetP and allow for transport of choline as well (Perez *et al*, 2011b). This lipid interaction is only resolved in the one chain which has a symmetry molecule packing close to its head group (Supplementary Figure S10). To investigate a possible impact of lipid interaction with the glycine-rich stretch on transporter activity and regulation as suggested in the structure, we exchanged Met150 against isoleucine and phenylalanine. Subsequent (^{14}C) betaine uptake in *E. coli* MKH13 cells was measured in dependence to the external osmotic stress (Figure 4C). While the Met150PheIle152Ala double mutant showed only a slightly altered osmoprofile, Met150Ile requires significantly higher osmolalities for maximal activity. Being part of the glycine-rich unwound stretch of TM1′, we compared the effects of the methionine mutations to alanine scanning mutations of the glycine motif (Perez *et al*, 2011b). The effect of the introduced phenylalanine at position 150 on regulation in BetP in particular is comparable to that of Gly153Ala (Figure 4C; Perez *et al*, 2011b). We speculate that both mutations, Met150Phe and Gly153Ala, result in a decrease in flexibility of the stretch itself, affecting substrate binding and release during the alternating access cycle (Perez *et al*, 2012). In fact, the affinity for betaine is strongly decreased in Met150PheIle152Ala by a factor of 100 (Supplementary Table S2), although the osmoprofile is nearly like the one of the WT. Interestingly, the exchange of Met150 against isoleucine only alters the apparent Km values by a factor of 2 (Supplementary Table S2), whereas the osmoprofile is significantly shifted (Figure 4C). While these mutations could possibly alter local protein–protein interactions around the unwound stretch, they could also directly affect the observed local protein–lipid interaction. Due to its length and hydrophobic nature isoleucine may complement the hydrophobic cleft for lipid binding and favour a stronger interaction with the acyl chain than methionine or a bulky phenylalanine. We therefore presume that the distinct architecture provided by the glycines and methionine needs to be maintained for the plasticity required in stretch movements during the transport cycle and suggest that the lipid–protein interaction of L7 with the catalytic core has an impact on regulation in BetP.

Lipid association may affect conformational states in BetP

Although each protomer in the trimer presented here adopts similar transport states, their C-terminal helices reveal an asymmetry that has been consistently observed in all crystal structures of BetP obtained thus far. Asymmetry in BetP either presents as in this case, only at the level of C-terminal orientation (and Ressl *et al*, 2009) or additionally also in the form of functionally asymmetric trimers, where each chain adopts a different state in the transport cycle (Tsai *et al*, 2011; Perez *et al*, 2012). In this higher resolution structure, we observe yet another level of asymmetry coming from the resolved lipid-binding sites (Figure 5C). Each chain of BetP shows different amounts of lipids associated with it, although each of them is functionally in the same state. While the improved resolution in comparison to the previously reported BetP structures enabled identification of these lipids, some densities at sites equivalent to the central lipids were seen in lower resolution structures. The

most prominent density from these was that for lipid L4 (Supplementary Figure S8).

Since spots of probable lipid-like density were present in the lower resolution structures, we attempted to use lipid site information from this higher resolution structure to refine two asymmetric trimers of BetP, which presented the outward and the closed conformations (Perez *et al*, 2012) (Supplementary Figure S8). Densities for four central lipids were seen in the trimer with the outward states while only one central lipid was partially resolved in the trimer with the closed states. Annular lipid sites do not appear to be occupied in the outward and closed states. While this could be an indication of different occupancies of lipids in different conformations of the transport cycle, we cannot rule out other important factors like differences in resolution of the structures and differences arising during expression or crystallization conditions themselves. It is possible that we could detect such a large amount of lipid densities in the functional state-symmetric trimer structure because all protomers adopt a single conformation. This suggests a link between the transporter state and specific lipid–protein interactions in BetP. In the light of transport regulation in BetP, specific lipid interactions with structural elements involved in the alternating access mechanism might represent an elegant way to populate distinct transporter states contributing to inactivation or activation. A similar concept was proposed previously for LeuT (Mondal *et al*, 2013). MD simulations revealed that in LeuT lipid–protein interactions are different in the functionally distinct conformations (outward-open, occluded, inward-open) and that the differences are mainly connected to structural elements (e.g., TM1a), which play key roles in transport. That the membrane can play a key role in aiding smooth conformational state transitions was also proposed for sarco (endo) plasmic reticulum Ca^{2+}-ATPases, when small adaptations in protein side chains and helix tilts were observed in response to local membrane deformations (Sonntag *et al*, 2011).

Putative role of lipids in trimer assembly of BetP

The need for specific lipid association for correct protein and oligomeric assembly has been described in different proteins. A crucial structural dependence on the presence of PE lipids was reported for HorA, a multi-drug ABC transporter from *Lactobacillus brevis*, in which the orientation of TM helices was altered when native PE was replaced with PC lipids, thereby modulating its activity (Gustot *et al*, 2010). PG lipids are known to play a role in the proper folding of alpha helical membrane proteins (Seddon *et al*, 2008). The crystal structure of the bacterial potassium channel revealed the presence of PG lipids co-purified after extraction from *E. coli* membranes and they were found to be important in refolding the channel to a functional tetramer (Valiyaveetil *et al*, 2002).

Anionic lipids in the structure of BetP allude to a similar membrane mediated trimeric assembly. In the heterologous expression system *E. coli*, we assume that BetP is inserted in PG-enriched membrane domains as it was reported previously for the osmotic stress-regulated transporter ProP, which is expressed in cardiolipin-enriched poles of *E. coli* (Mileykovskaya, 2007; Romantsov *et al*, 2008). From the presented data, we consistently see central lipids bound within the trimer, suggesting an important role for these lipids as cofactors during trimeric assembly. We suggest that lipids around each chain are required for stabilization of the monomeric structure and increase the number of specific electrostatically favourable interactions available for chain–chain interactions (Figure 5C). We observe that lipid binding is typically pronounced in the inward-facing conformation. Therefore, the asymmetrically occupied lipid binding sites if originating already during assembly may also provide a seeding point for forming asymmetric functional trimers, as seen in structures reported previously (Perez *et al*, 2012).

Lipid interactions are putatively involved in stress sensing

Trimerization in BetP also essentially involves the amphipathic helix h7 (Perez *et al*, 2011a), which in turn is associated with the periplasmic interaction networks. This helix is composed of a total of 7 Ser, Thr and Gly residues on its polar face and a single Arg residue. It also possesses a well-developed hydrophobic face that is seen to coordinate lipid acyl chains in the structure of the substrate-free trimer (Figure 2B; Supplementary Figure S9). Similar helices are present in another osmotic stress-regulated transporter, OpuA, where the amphipathic helix was found to require a well-developed hydrophobic face for its function, although here it is assumed to interact with other domains within the protein and not the bilayer itself (Gul *et al*, 2012). Incidentally, h7 in BetP harbours some of the characteristics of a general motif for sensing changes in the bilayer curvature, called the Amphipathic Lipid Packing Sensor (ALPS or ArfGAP1 lipid packing sensor) motif (Supplementary Figure S12; Mesmin *et al*, 2007). Because of the lack of many charged residues on their polar surface these amphipathic helices associate with the membrane mainly by their hydrophobic face and are therefore highly sensitive to changes in membrane curvature (Mesmin *et al*, 2007). Activation by sensing membrane tension and possible curvature changes has previously been reported in mechanosensitive channels (MscS/MscL), the emergency valves of bacterial cells during hypoosmotic stress (Wang *et al*, 2008; Nomura *et al*, 2012). Membrane curvature changes are also inevitable in hyperosmotic stress. Sensing and responding to such changes as a direct effect of stress would be a tempting scenario for BetP as well. Indeed, a possible difference in membrane curvature is indirectly observed when the curvature suggested by the resolved lipids and inter-chain distances in the X-ray structure are compared to that from 3D fitting on an 8 Å 2D map of BetP (Tsai *et al*, 2011). A putative curvature sensing property of h7 would be ideal to transduce membrane-related stimuli through the transporter. Certainly experimental proof for h7 being a curvature sensor still has to be adduced. However, in this speculative scenario lipids would be the transducing link between the two putative osmosensors, h7 and the C-terminal domain, one sensing the membrane stress stimulus, the other sensing internal K^+ concentration.

Materials and methods

N-terminal *strepII-betp* in an IBA7 vector, BetPΔN29EEE44/45/46AAA, was heterologously expressed in *E. coli* DH5αmcr cells. The protein was solubilized from isolated membranes using β-dodecyl-maltoside and purified by affinity and size-exclusion chromatography as previously described (Rübenhagen *et al*, 2000). A variation in the detergent exchange step on the

StrepTactin column was introduced in the protocol by exchanging with 1.2% Cymal-5 instead of the earlier established 0.6% Cymal-5. Crystals of BetP were grown by vapour diffusion at 18°C by mixing a 1:2 volume of protein (~12 mg/ml) and reservoir solution containing 100 mM 3Na-Citrate (pH 5.4–5.5), 300 mM NaCl, 20–21% PEG400. BetPΔN29EEE44/45/46AAA single crystal yielded isotropic diffraction to 2.7 Å. XDS (Kabsch, 1993) was used for 3D data processing and the structure was determined by molecular replacement (McCoy *et al*, 2007) using the BetP trimer (PDB entry 2WIT). No non-crystallography symmetry (NCS) was imposed during refinement steps to account for possible asymmetry in the structure. Multiple iterations of refinement and manual model building with PHENIX (Terwilliger *et al*, 2008) (version 1.6) and COOT (Emsley and Cowtan, 2004) (version 0.7), respectively, were used to arrive at the final deposited model. Data processing and refinement statistics are reported in Supplementary Table S1. Citrate and lipid moieties were positioned only after clear positive peaks in the Fo-Fc maps and distinguishable features in the 2Fo-Fc maps were observed after several refinement rounds.

Lipid species bound to solubilized protein after purification was analysed by comparing with known lipid standards on pre-coated HPTLC silica gel plates. A chloroform:methanol:water (13:7:0.8) solvent system was used to separate in one dimension. An acetone:methanol:acetic acid:water:chloroform (2:1:1:0.5:5) solvent system was used to differentiate between CL and PG in one dimension. Lipid visualization was done using iodide vapours followed by a molybdenum blue spray reagent to specifically stain phospholipids. Uptake of labelled betaine was measured in *E. coli* MKH13 cells, started by adding 250 μM [^{14}C] betaine upon an osmotic shock adjusted with KCl. All figures of the structure were made using the PyMOL Molecular Graphics System.

Accession code

Coordinates and structure factors for the structure presented here (PDB entry 4C7R) have been deposited into the Protein Data Bank.

Supplementary data

Supplementary data are available at *The EMBO Journal* Online (http://www.embojournal.org).

Acknowledgements

We are thankful to Reinhard Krämer, Werner Kühlbrandt, Lucy Forrest and Marcus Becker for careful reading of the manuscript and valuable discussions and suggestions. We thank the beam line staff of id29 at ESRF in Grenoble/FR and the team at PXII, SLS in Villigen/CH, especially Anuschka Pauluhn and Martin Fuchs, for excellent facilities and assistance during data collection and crystal testing. This work was supported by the International Max-Planck Research School, Frankfurt, and by the SFB-807 (Transport and communication across biological membranes) of the Deutsche Forschungsgemeinschaft (DFG).

Author contributions: CK performed crystallization; CK and ÖY performed collection, processing and refinement of data; CK and CZ analysed the data; ESS, RMG and CP performed mutations and activity measurements in cells; CK and ESS performed TLC analysis; CZ directed the research; CK and CZ wrote the manuscript and all authors commented on it.

Conflict of interest

The authors declare that they have no conflict of interest.

References

Emsley P, Cowtan K (2004) Coot: model-building tools for molecular graphics. *Acta Crystallogr D* **60:** 2126–2132

Forrest LR, Kramer R, Ziegler C (2011) The structural basis of secondary active transport mechanisms. *Biochim Biophys Acta* **1807:** 167–188

Gärtner RM, Perez C, Koshy C, Ziegler C (2011) Role of bundle helices in a regulatory crosstalk in the trimeric betaine transporter BetP. *J Mol Biol* **414:** 327–336

Gul N, Schuurman-Wolters G, Karasawa A, Poolman B (2012) Functional characterization of amphipathic alpha-helix in the osmoregulatory ABC transporter OpuA. *Biochemistry* **51:** 5142–5152

Gustot A, Smriti, Ruysschaert JM, Mchaourab H, Govaerts C (2010) Lipid composition regulates the orientation of transmembrane helices in HorA, an ABC multidrug transporter. *J Biol Chem* **285:** 14144–14151

Hoischen C, Krämer R (1990) Membrane-alteration is necessary but not sufficient for effective glutamate secretion in Corynebacterium Glutamicum. *J Bacteriol* **172:** 3409–3416

Kabsch W (1993) Automatic processing of rotation diffraction data from crystals of initially unknown symmetry and cell constants. *J Appl Crystallogr* **26:** 795–800

Krämer R, Morbach S (2004) BetP of Corynebacterium glutamicum, a transporter with three different functions: betaine transport, osmosensing, and osmoregulation. *Biochim Biophys Acta* **1658:** 31–36

Lee AG (1998) How lipids interact with an intrinsic membrane protein: the case of the calcium pump. *Biochim Biophys Acta* **1376:** 381–390

Lee AG (2004) How lipids affect the activities of integral membrane proteins. *Biochim Biophys Acta* **1666:** 62–87

Lee AG (2011) Lipid-protein interactions. *Biochem Soc Trans* **39:** 761–766

Matyash V, Liebisch G, Kurzchalia TV, Shevchenko A, Schwudke D (2008) Lipid extraction by methyl-tert-butyl ether for high-throughput lipidomics. *J Lipid Res* **49:** 1137–1146

McCoy AJ, Grosse-Kunstleve RW, Adams PD, Winn MD, Storoni LC, Read RJ (2007) Phaser crystallographic software. *J Appl Crystallogr* **40:** 658–674

Mesmin B, Drin G, Levi S, Rawet M, Cassel D, Bigay J, Antonny B (2007) Two lipid-packing sensor motifs contribute to the sensitivity of ArfGAP1 to membrane curvature. *Biochemistry* **46:** 1779–1790

Mileykovskaya E (2007) Subcellular localization of Escherichia coli osmosensory transporter ProP: focus on cardiolipin membrane domains. *Mol Microbiol* **64:** 1419–1422

Mondal S, Khelashvili G, Shi L, Weinstein H (2013) The cost of living in the membrane: a case study of hydrophobic mismatch for the multi-segment protein LeuT. *Chem Phys Lipids* **169:** 27–38

Morbach S, Krämer R (2003) Impact of transport processes in the osmotic response of Corynebacterium glutamicum. *J Biotechnol* **104:** 69–75

Nomura T, Cranfield CG, Deplazes E, Owen DM, Macmillan A, Battle AR, Constantine M, Sokabe M, Martinac B (2012) Differential effects of lipids and lyso-lipids on the mechanosensitivity of the mechanosensitive channels MscL and MscS. *Proc Natl Acad Sci USA* **109:** 8770–8775

Ott V, Koch J, Spate K, Morbach S, Kramer R (2008) Regulatory properties and interaction of the C- and N-terminal domains of BetP, an osmoregulated betaine transporter from Corynebacterium glutamicum. *Biochemistry* **47:** 12208–12218

Oursel D, Loutelier-Bourhis C, Orange N, Chevalier S, Norris V, Lange CM (2007) Lipid composition of membranes of Escherichia coli by liquid chromatography/tandem mass spectrometry using negative electrospray ionization. *Rapid Commun Mass Spectrom* **21:** 1721–1728

Özcan N, Ejsing CS, Shevchenko A, Lipski A, Morbach S, Kramer R (2007) Osmolality, temperature, and membrane lipid composition modulate the activity of betaine transporter BetP in Corynebacterium glutamicum. *J Bacteriol* **189:** 7485–7496

Özcan N, Kramer R, Morbach S (2005) Chill activation of compatible solute transporters in Corynebacterium glutamicum at the level of transport activity. *J Bacteriol* **187:** 4752–4759

Perez C, Khafizov K, Forrest LR, Kramer R, Ziegler C (2011a) The role of trimerization in the osmoregulated betaine transporter BetP. *EMBO Rep* **12:** 804–810

Perez C, Koshy C, Ressl S, Nicklisch S, Kramer R, Ziegler C (2011b) Substrate specificity and ion coupling in the Na+/betaine symporter BetP. *EMBO J* **30:** 1221–1229

Perez C, Koshy C, Yildiz O, Ziegler C (2012) Alternating-access mechanism in conformationally asymmetric trimers of the betaine transporter BetP. *Nature* **490:** 126–130

Perozo E, Kloda A, Cortes DM, Martinac B (2002) Physical principles underlying the transduction of bilayer deformation forces during mechanosensitive channel gating. *Nat Struct Biol* **9:** 696–703

Peter H, Burkovski A, Krämer R (1996) Isolation, characterization, and expression of the Corynebacterium glutamicum betP gene, encoding the transport system for the compatible solute glycine betaine. *J Bacteriol* **178:** 5229–5234

Phillips R, Ursell T, Wiggins P, Sens P (2009) Emerging roles for lipids in shaping membrane-protein function. *Nature* **459:** 379–385

Poolman B, Spitzer JJ, Wood JM (2004) Bacterial osmosensing: roles of membrane structure and electrostatics in lipid-protein and protein-protein interactions. *Biochim Biophys Acta* **1666:** 88–104

Quick M, Shi L, Zehnpfennig B, Weinstein H, Javitch JA (2012) Experimental conditions can obscure the second high-affinity site in LeuT. *Nat Struct Mol Biol* **19:** 207–211

Ressl S, Terwisscha van Scheltinga AC, Vonrhein C, Ott V, Ziegler C (2009) Molecular basis of transport and regulation in the Na(+)/betaine symporter BetP. *Nature* **458:** 47–52

Romantsov T, Stalker L, Culham DE, Wood JM (2008) Cardiolipin controls the osmotic stress response and the subcellular location of transporter ProP in Escherichia coli. *J Biol Chem* **283:** 12314–12323

Rübenhagen R, Morbach S, Kramer R (2001) The osmoreactive betaine carrier BetP from Corynebacterium glutamicum is a sensor for cytoplasmic K+. *EMBO J* **20:** 5412–5420

Rübenhagen R, Ronsch H, Jung H, Kramer R, Morbach S (2000) Osmosensor and osmoregulator properties of the betaine carrier BetP from Corynebacterium glutamicum in proteoliposomes. *J Biol Chem* **275:** 735–741

Schiller D, Ott V, Kramer R, Morbach S (2006) Influence of membrane composition on osmosensing by the betaine carrier BetP from Corynebacterium glutamicum. *J Biol Chem* **281:** 7737–7746

Seddon AM, Lorch M, Ces O, Templer RH, Macrae F, Booth PJ (2008) Phosphatidylglycerol lipids enhance folding of an alpha helical membrane protein. *J Mol Biol* **380:** 548–556

Sonntag Y, Musgaard M, Olesen C, Schiott B, Moller JV, Nissen P, Thogersen L (2011) Mutual adaptation of a membrane protein and its lipid bilayer during conformational changes. *Nat Commun* **2:** 304

Terwilliger TC, Grosse-Kunstleve RW, Afonine PV, Moriarty NW, Zwart PH, Hung LW, Read RJ, Adams PD (2008) Iterative model building, structure refinement and density modification with the PHENIX AutoBuild wizard. *Acta Crystallogr D* **64:** 61–69

Tsai CJ, Khafizov K, Hakulinen J, Forrest LR, Kramer R, Kuhlbrandt W, Ziegler C (2011) Structural asymmetry in a trimeric Na+/betaine symporter, BetP, from Corynebacterium glutamicum. *J Mol Biol* **407:** 368–381

The PyMOL Molecular Graphics System, Version 1.3, Schrödinger, LLC.

Valiyaveetil FI, Zhou YF, Mackinnon R (2002) Lipids in the structure, folding, and function of the KcsA K+ channel. *Biochemistry* **41:** 10771–10777

van der Heide T, Stuart MCA, Poolman B (2001) On the osmotic signal and osmosensing mechanism of an ABC transport system for glycine betaine. *EMBO J* **20:** 7022–7032

Walz T, Hirai T, Murata K, Heymann JB, Mitsuoka K, Fujiyoshi Y, Smith BL, Agre P, Engel A (1997) The three-dimensional structure of aquaporin-1. *Nature* **387:** 624–627

Wang H, Elferich J, Gouaux E (2012) Structures of LeuT in bicelles define conformation and substrate binding in a membrane-like context. *Nat Struct Mol Biol* **19:** 212–219

Wang WJ, Black SS, Edwards MD, Miller S, Morrison EL, Bartlett W, Dong CJ, Naismith JH, Booth IR (2008) The structure of an open form of an *E. coli* mechanosensitive channel at 3.45 angstrom resolution. *Science* **321:** 1179–1183

Wood JM (1999) Osmosensing by bacteria: signals and membrane-based sensors. *Microbiol Mol Biol R* **63:** 230–262

Yoshimura K, Sokabe M (2010) Mechanosensitivity of ion channels based on protein-lipid interactions. *J R Soc Interface* **7**(Suppl 3): S307–S320

Zhao Y, Terry DS, Shi L, Quick M, Weinstein H, Blanchard SC, Javitch JA (2011) Substrate-modulated gating dynamics in a Na+-coupled neurotransmitter transporter homologue. *Nature* **474:** 109–113

Zhou Y, Morais-Cabral JH, Kaufman A, MacKinnon R (2001) Chemistry of ion coordination and hydration revealed by a K+ channel-Fab complex at 2.0 A resolution. *Nature* **414:** 43–48

Ziegler C, Bremer E, Kramer R (2010) The BCCT family of carriers: from physiology to crystal structure. *Mol Microbiol* **78:** 13–34